Journal of Scientific & Industrial Research
Vol. 82, April 2023, pp. 475-484
DOI: 10.56042/jsir.v82i04.70789

Land Use/Land Cover Change and Environmental Impact Analysis of Ramgarh-Naudiha Region in Uttar Pradesh, India through Geospatial Technology

Debiprasad Karmakar[1,4]*, Vartika Singh[2], Raghvendra Singh[1], Lalit Kumar Sharma[3] & Swapankumar Ghosh[3,5]*

[1]Amity Institute of Geo-Informatics and Remote Sensing, [2]Amity Institute of Global Warming and Ecological Studies, Amity University, Noida 201 301, Uttar Pradesh, India

[3]CSIR-Central Glass & Ceramic Research Institute, Khurja Centre 203 131, Uttar Pradesh, India

[4]CSIR-Recruitment and Assessment Board, CSIR Complex, Library Avenue, New Delhi 110 012, India

[5]Department of Chemistry, West Bengal State University, Berunanpukuria, Kolkata 700 126, West Bengal, India

Received 23 January 2023; revised 02 March 2023; accepted 03 March 2023

Rapidly changing LULC scenario with growing population is of great concern in the modern world. The present study was undertaken to evaluate the changes in LULC pattern in Ramgarh-Naudiha region of Sonbhadra district, UP, over 20 years during 1998–2018 using datasets from the Landsat Thematic Mapper (TM) 5 and Landsat 8 (OLI/TIRS) satellites. LULC map for the chosen period has been generated by unsupervised classification with maximum likelihood algorithm. Results indicate that the study area is vulnerable to such LULC changes due to its sensitive geographic location. It is found that the major changes did happen in agriculture, forest, wasteland and water bodies. Agriculture and Forest areas have decreased by ~2 and 6.56% respectively in the study period. The wastelands had increased fast from 5.08% in 1998 to 18.87% in 2018 at the cost of the forest cover and agricultural land respectively. In 1998, water bodies were 7.49%, whereas, it has decreased to 2.04% in 2018. On the contrary, urban fringe area has grown from 0.33% in 1998 to 0.49% in 2018 especially due to population growth. The present study concludes that this LULC analysis will increase awareness and help in taking necessary action in appropriate land use planning and management.

Keywords: GIS, Land use and land cover, NDVI, Remote sensing, Unsupervised classification

Introduction

Human population has grown from 2.6 billion in 1950 to 7.7 billion today, and may cross 9.7 billion by 2050. It will have increased demand for food, water, energy, housing etc. To meet these demands, uncontrolled exploitation of natural resources have deteriorated the surface of Earth significantly over the past centuries.[1] Several socioeconomic, ecological and political factors, like industrial growth, population growth, and government decisions affect Land-Use/Land-Cover (LULC) changes which may have positive or negative effects on the natural resources.[2] One of the main negative effects of LULC changes is deforestation which has caused a series of environmental effects, like increased CO_2 level, changing earth's climate, surface ecological and biophysical characteristics.[3,4] So it is important to understand the negative impacts of LULC change and their key driving factors. The distribution of LULC changes vary in space and time depending on the human social behaviour and its physical characteristics. Natural resources like minerals have beneficial impacts on socioeconomics of the entire region. Geologically Sonbhadra district consisting of Dudhi granitoid in Vindhyan super group under Mahakoshal group, has rich mineral resources. The minerals are Limestone for production of cement, Dolomite as well as Clay, Calcite and Silimanite.[5] Uncontrolled mining activities and the population growth in Sonbhadra district is reported to have negative impact on the environment[5] as envisaged by the fast increase in wasteland and decrease in agricultural land which may have happened due to lack of preplanning. The clays available there have also been used for making bricks for housing. The present challenge is to identify the adverse effects of deforestation and mining activities on environment in a region and model them. Uncontrolled mining activities directly affect natural resources and have potential to harm the surface biophysical characteristics.[6] The effects on surface biophysical characteristics e.g., surface temperature, albedo, water content, vegetation etc. vary with type of exploration,

*Authors for Correspondence
E-mail: swapankumar.ghosh2@mail.dcu.ie; dpkcgcri@gmail.com

extraction and processing methods, and depend upon types of minerals, location, and associated parameters.[7]

Satellite images are conveniently employed to study the surface biophysical characteristics after mining and anthropogenic activities in that area. Satellite imaging is multi-temporal and multi-spectral, and canopy large areas.[8] It has several advantages for exploring the type, amount and site of LULC change and its effect on the surface biophysical properties over vast areas.[8–10] In a previous study, the authors have expressed the environmental impact in Sonbhadra district in the matrix method with a numerical impact value index, which has several limitations.[5]

Satellite images were employed to find the effects of mining activities on the surface biophysical characteristics and were focused on assessing the LULC changes from the trend of mining areas. Normalised Difference Vegetation Index (NDVI) is a very useful parameter in the study of surface biophysical characteristics in the surrounding areas of extensive mining and anthropogenic activities and is the most important and applicable indicator in modelling the surface biophysical characteristics.[11]

The clay available in the area has been under-utilized for making building bricks. To the best of our knowledge, there is only one published report which indicated fast population growth and urbanization by converting agricultural lands and filling water bodies in the Ramgarh-Naudiha area of Sonbhadra district with no predictive solution.[5] With this background, the current study was undertaken in the Ramgarh-Naudiha Region of Sonbhadra district to estimate the biophysical indicators on the environment change like vegetation, wastelands, water bodies etc. over time through Geospatial Technology. The LULC has been generated from the satellite images of the study area over a period of twenty years (1998–2018) and evaluated its impacts on the surface by using an unsupervised classification algorithm. The NDVI values of the study area have also been determined to see the effect on the vegetation. Accuracy assessment of both the LULC and NDVI changes were administered to assess the accuracy of the classification. Combining remotely sensed information (signal) within the optical and thermal ranges of the electromagnetic spectrum from surface, supported by on field study, can increase the accuracy in modeling the complex interactions in surface biophysical characteristics.[12] This is useful and critical for management and planning in predicting the future trends and its negative effects.

Materials and Methods

Study Area

Sonbhadra is the only district in India which shares its border with four states. Madhya Pradesh is situated in its west, Chhattishgarh in the south, Jharkhand to the south-east and Bihar is in the north-east. Area of Sonbhadra district is 6788 km^2 and situated in the south-east corner of Uttar Pradesh. Robertsganj is the district headquarters of Sonbhadra. It is in the industrial zone and it has minerals like bauxite, limestone, coal, gold etc. It is called the “Energy Capital of India” because of many power plants there. The district is administratively divided into 3 tehsils namely Robertsganj, Dudhi and Ghorawal which are further divided into 8 development blocks. In this effort, the study area lies south of the Son River flowing from west to east near Ramgarh-Naudiha in the Sonbhadra district of Uttar Pradesh (Latitude 24°28’N to 24°23’N, Longitude 83°12’E to 83°24’E) (Fig. 1). The drainage in the study area constitutes the rivers Son, Rihand, Kanhar, Karmanasha, Gaghar and Belan and their tributaries. Near Kalighat, Son enters the area, flows for about 60 km towards east and leaves the area about 15 km north-east of Kon and enters Bihar. The Son River forms a deep valley ~12–15 km wide. It is a part of the Kaimur plateau with undulated land and separates from the Son valley by a sharp line in the south.[13]

Data and Pre-processing

The satellite images of Landsat 5 and 8 were used in this study for LULC and NDVI mapping. The acquired images in Geo-Tiff format were geo-referenced in the World Geodetic System (WGS84) datum, and projected in the Universal Transverse Mercator (UTM, zone 44 N). The absence of cloud cover and no rain two days prior to the satellite’s passage was considered while selecting the satellite images during 1998 and 2018 (Table 1).

In order to provide the training and test data for image classification and accuracy assessment of extracted LULC maps, Landsat false colour composite images were utilised.

Remote Sensing

Satellite remote sensing has immense potential in ensuring a synoptic view of the landscape at the local to the global level. Furthermore, satellite-based

Table 1 — Satellite details for imagery of the study area

Sl. No.	Satellite	Sensor	Spectral bands	Month/Year of acquisition	Path/Row	Av. cloud cover (%)
1	Landsat 5	TM	7	January 16, 1998	142/43	4.1
2	Landsat 8	OLI/TIRS	11	April 13, 2018	142/43	2

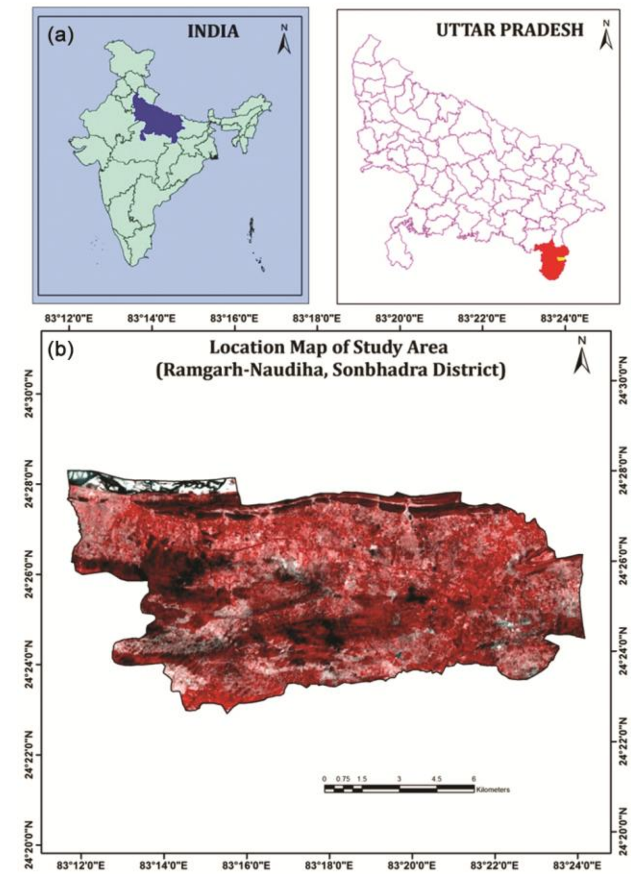

Fig. 1 — (a) Location map in UP, India, and (b) Landsat 8 satellite image of the study area

remote sensing sensors can capture the spectrum in visible and other ranges and can split the whole electromagnetic spectrum into various bands. This permits the extraction of data from the earth's surface about its variations in the reflective property to the different electromagnetic wavelengths.[14] GIS can provide information on natural as well as on anthropogenic induced resources in spatial domains and enables decision making and execution of policies. Remote sensing is an important tool of land imaging science as it enables observations across larger areas of Earth's surface than is possible by ground-based observations. This is often accomplished by the use of cameras, multi-spectral scanners, RADAR and LiDAR sensors mounted on air- and space-borne objects enabling aerial photographs, satellite imagery, and data from RADAR and LiDAR sensors. Remote sensing data vary from the very high-resolution datasets procured at required intervals to the extent no larger than a single state or province (by aerial photography, imaging, LiDAR, and high-resolution satellite sensors like CartoSat, IKONOS, and Quick-bird), to regional datasets collected at regular intervals from satellites (e.g., LISS III, Landsat and SPOT), to lower-resolution (>250 m) datasets now produced across the whole Earth on a daily basis (e.g., MODIS). The temporal dynamics of the earth's surface by satellite-assisted data capture have given us a crucial tool to study the variations in land use and land cover over a period of time. Hyperspectral imaging sensors captures numerous spectral bands at varying wavelengths to characterise the objects present in the surface of Earth. These imaging systems generate large volumes of data consist of rich information about the scene which is more detailed than the conventional imaging systems like multispectral sensors.[15]

The changes within the LULC manifested as a function of the changes either natural or manmade, have an impact on the reflectance patterns of incident radiation due to the consequent changes in the vegetative cover, soil cover, or the varied modifications of the earth's surface.[16] Since the changes in LULC are more or less unidirectional, without much scatter, it is rather safe to extrapolate the changes in spatial domains to calculate the rate of changes. Geographical Information System (GIS) is a very important and powerful tool in which spatial information can be stored, organized, and retrieved during a user-friendly environment. The conjunction of satellite remote sensing and also as an ancillary data in a GIS environment, combined with the Global Positioning System (GPS) data, is a potential tool for environmental management.

Modelling LULC Change

Modelling the LULC change requires generation of scenarios. The relationship of the people with the land has the same origin as their evolution–the ability of human to modify their surroundings to suit themselves. Land use change may be a locally pervasive and globally significant ecological phenomenon. These changes in land use trend have significant implications for future changes of the earth's climate and, in turn, greater implications for subsequent LULC change. The surface heat and moisture content depend considerably on LULC which, in turn, affect atmospheric stability. Simulations of the plausible human-influenced landscape changes following man-made activities may reveal strategic policies that ought to be implemented to improve the environment. Understanding the spatial dynamics of LULC change has been a challenge for geospatial scientists and so far, there is not a single robust model which can demonstrate the LULC dynamics of a region. Historical land use patterns including the current trends in a region are used to model future land use.

Overview of Normalised Difference Vegetation Index (NDVI)

Greenness or photosynthetic activity is an index of plant referred to as NDVI. It is easily calculated from the satellite image-based proxy for vegetation productivity.[17] NDVI may be a simple numerical indicator[18] which is related to Photo-synthetically Active Radiation (PAR) and basically measures the capability of leaves[19] and gives a measure of the land surface's vegetative cover over wide areas. This index shows direct correlation with photosynthetic activity, vegetation cover, biomass, and Leaf Area Index (LAI).[20] The NDVI algorithm is computed by subtracting the red reflectance values from the near-infrared and divided it by the sum of near-infrared and red bands.[21] The function is

$$NDVI = \frac{(NIR-RED)}{(NIR+RED)} \quad \text{... (1)}$$

where, NIR represents the spectral reflectance in near infrared band while RED represents red band. NDVI values range from –1 to 1. Barren areas of rock, sand, snow, cloud etc. indicate very low value of NDVI. Shrub and grassland are represented by moderate values while temperate and tropical rainforests indicate high value. Bare soil is assigned with NDVI values close to 0 and water bodies are represented with negative NDVI values.[22,23] The NDVI technique is an easy tool to implement and simple to interpret, but there are many flaws. Satellite-based NDVI are influenced by several non-vegetation factors: atmospheric conditions (e.g., clouds, aerosols and water vapour), satellite geometry, calibration (view and solar angles), and soil backgrounds and crop canopy.[24–26] Similarly, cloud shadows affect NDVI values and cause misinterpretation.

Software Used

Data processing has been done using ERDAS IMAGINE 9.2 and Arc GIS 10.1 software. Corrections were incorporated to remove atmospheric effects by the histogram equalize method and geo-referenced using 30 ground control points derived from the topographical maps of 1:50,000 scale of the study area. They were projected to an Universal Transverse Mercator (UTM) coordinate system, Datum WGS 1984, zone 45 North using 1:50,000 topographic map of the study area. By the band combination Standard False Colour Composites (FCC) are prepared from the satellite images. The study area is extracted from the FCC through subset and NDVI prepared using ERDAS IMAGINE 9.2 software. Separation of every band is essential to create NDVI from the multispectral remote sensing image. For the extraction of vegetation features, NDVI method is employed at four different thresholds e.g., 0.2, 0.3, 0.4 and 0.6 through the observation of maximum and minimum NDVI values. The ultimate layout map of three different categories of NDVI values is created by manual method using Arc GIS 10.1 software. Finally, the NDVI values were categorized into three different classes (areas) with low (0.2–0.3), medium (0.3–0.4) and high (>0.4) vegetation density on the ranges of NDVI of both 1998 and 2018 images. Shrub and grassland are represented by 0.2–0.3 NDVI value, 0.3–0.4 denotes sparse and unhealthy forest, whereas >0.4 NDVI value indicates dense and healthy vegetation. Here, we used remote-sensing techniques to examine the forest loss over the last 20 years.

This study demonstrates that exploiting a free archive of Landsat data, and it's processing through two softwares, provides an accurate approach to mapping and analyzing changes in land cover over time which will be used as a guide to land management and policy decisions. ERDAS software was employed in LULC classification and ArcGIS software was used to extract NDVI index, Unsupervised Classification, and establish necessary maps. Microsoft Office Excel was employed in statistical analysis as well as established the necessary diagrams. The ArcGIS software and free/open-source QGIS software were exploited to execute land cover analysis, using the Unsupervised Classification technique. Subsequently, the accuracy assessment test was administered for the selected software.

Data Preparation

By maximum likelihood algorithm, LULC maps were worked out by using the unsupervised classification method. Applying a multi-spectral unsupervised classification algorithm to Landsat sensor data Land cover map for the selected years is generated. Landsat 5 (TM) and Landsat 8 (OLI/TIRS) satellite images have seven and eleven bands respectively which were converted to an image by using composite bands.[27] For unsupervised classification, the processing of basic methods like composite band, copy raster, remove clouds and mosaic to new raster, extract by mask and maximum likelihood images classification were carried out. The processes were performed by ArcMap 10.1 software (Fig. 1b). The copy raster features were removed from the background of images for rendering a transparent background. This section was pre-processed for image classification. Haze reduction was performed in this section. For this study, image enhancement technique has been preferred for histogram equalisation. Cloud cover and haze condition were acceptable because it is zero in all images. To develop an accurate aerial representation of the study area, the image mosaic to new raster using ArcMap 10.1 software was created from the Landsat images. Mask tool was used for cutting the desired location.

Images Classification

In this study, images were classified into five major classes; Agriculture, Built-up, Forest, Wastelands and Water bodies. In this study, standard "false colour" composite was used for Landsat 5 TM satellite images which include 2, 3, 4 bands. This combination provides a "natural-like" rendition. Healthy vegetation was bright green, grasslands appeared green, pink areas were barren soil, sparsely vegetated areas appeared orange and brown, water was blue and urban areas appeared in varying shades of magenta. Landsat 8 TM produces false-colour composite (3, 4, 5) which repeats near what human eye can see. In this case sound vegetation appears green, and greenery is darker. Urban highlights appear white and dim whereas water is dull blue or dark. To train for selecting each LULC categories, images with relatively significant number of pixels were selected in this study. Finally, the maximum likelihood unsupervised image classification method was applied by using ArcGIS software.

Accuracy Assessment

Accuracy assessment was done in terms of user accuracy, producer accuracy, overall accuracy and Kappa Coefficient. About 50 random points were created and the minimum allowance distance was set at 30 m for each class. They were measured using Eqs 2–4.[(28)] User accuracy was measured using Eq. (2).[(28)]

$$User\ Accuracy = \frac{number\ \ of\ correct\ \ points\ \ (value\ )}{The\ row\ \ total\ \ (value\ )} \times 100 \quad \text{... (2)}$$

Producer accuracy was measured using Eq. (3):

$$Producer\ Accuracy = \frac{Number\ \ of\ correct\ \ points\ \ (value\ )}{The\ coloumn\ \ total\ \ (value\ )} \times 100 \quad \text{... (3)}$$

The overall accuracy was measured using Eq. (4):

$$Overall\ Accuracy = \frac{Number\ \ of\ total\ correct\ \ points\ \ (value\ )}{The\ number\ \ of\ points\ \ (value\ )} \times 100 \quad \text{... (4)}$$

The Kappa Coefficient, K was used as a measure of agreement between model predictions and reality[29] or to ascertain if the values comprised in an error matrix represent a result significantly better than random.[30] The applied Kappa coefficient values were calculated using by following Eq. (5)[(28,29)]:

$$K = \frac{N\sum_{i=1}^{r} x_{ij} - \sum_{i=1}^{r}(x_i \times x_j)}{N^2 - \sum_{i=1}^{r}(x_i \times x_j)} \times 100 \quad \dots (5)$$

where, N = total number of observations in matrix, x_{ij}= number of observations in row i, column j, x_i = total number of observations in row i, x_j = number of observations in column j and r = number of rows in error matrix.

Accuracy assessment is a valuable step in the remote sensing data processing. The actuality of the resulting output to a user is established by reference or 'ground truthing' data to support.[31] The errors of commission that illustrate the possibility of a classified data matching the land cover type of its similar real-world geographic location are measured by user accuracy. Producer's accuracy is measured errors of omission, which is an assessment of how well real-world land cover types can be classified. The overall accuracy of the classified image is compared to how each of the pixels is classified against the demonstrated land cover established from their consisted ground truth data.[29]

Producer's Accuracy

The probability of correctly classifying a pixel in a category of image is defined as the Producer's

Accuracy. The values in the column accuracy are the Producer Accuracy of the image.

User's Accuracy

The probability of finding the classified pixel on the image of that category on ground is defined as the User's Accuracy. The values in row reliability in the classified image are the User's Accuracy.

Overall Accuracy

In the classified image when all the classes found are accepted visually in the entire image, then it demonstrates its overall accuracy. The collective accuracy of the map for all classes explains the overall accuracy; the proportion of pixels correctly classified can be calculated.

Kappa Coefficient

Two other accuracies such as producer's and user's accuracies are traditionally calculated from error matrix. The results due to classification of pixels by these accuracy calculations are produced by chance, so the accuracy cannot be compared statistically. Thus, other accuracy assessment method is used, the Kappa analysis. In this, off-diagonal elements are incorporated as a product of the row and column marginal totals. Kappa analysis is a discrete multivariate technique and is used to assess classification accuracy from an error matrix and it generates a Kappa coefficient, which range between 0 and 1. Image classification is not complete unless its accuracy is assessed. In order to determine the accuracy of classification, sample test pixels are selected on the classified image and compared with ground truth reference data. Deciding the suitable sample size for test data and sampling scheme plays a key role in the assessment of classification accuracy.[32] In order to assess the accuracy of the classifications, overall accuracy is a standard criterion used (total number of sample points).[33]

The accuracy of NDVI is assessed by comparing the high-resolution Google earth images with the field data points. Ten random reference points were taken and digitised for each class for accuracy assessment. Subsequently, both the 1998 and 2018 NDVI maps were superimposed and the coordinate values were noted using GPS (Geographical Positioning System) in the field data where the vegetation has disappeared in 2018 from the study area and its surrounding. Accuracy level is calculated on the basis of Google image and field verification. To determine the relationship between LULC characteristics, NDVI index is used. High NDVI index values show high vegetation distribution in the study area. NDVI indices in residential, industrial and commercial areas are higher than that of water, river and lakes and lower than vegetation area. During summer and winter times in cities, the NDVI values differ widely. High NDVI is shown in red and orange background, which indicates the best time for plants to thrive, and cultivate.

Manual Classification

Before technological advancement, manual classification was the primary method to classify satellite images. The accuracy of the analysis is often affected by the compelling reasons if the investigator is familiar with the study area. This technique analyses satellite images utilizing signs of tone, surface, shape, and relationship to different land cover classes. Human mind can beat a computer in recognizing the image highlights. Manual grouping has the advantage of analyzing the satellite picture with a printed copy without a PC. Analyst knowledge and familiarity towards the field of study influence the efficiency and accuracy of the classification.

Results and Discussion

LULC Classification: Unsupervised Algorithm

Topography, type of rocks (hard or soft), and the slope of the land controls the drainage pattern of the land in the study area (Fig. 2). Applying maximum likelihood and multi-spectral unsupervised classification algorithm, LULC maps for the period 1998–2018 were prepared with twenty years interval (Fig. 3). In 1998, water bodies were 7.49% (1077 ha), whereas, it decreased to almost 2.04% (293 ha) in

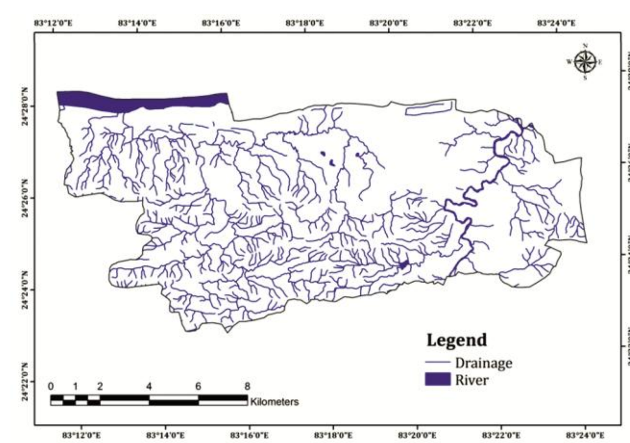

Fig. 2 — Drainage map of Ramgarh-Naudiha, Sonbhadra district, Uttar Pradesh

Table 2 — Land use and land cover of the study area using unsupervised classification for 1998 and 2018

	Unsupervised (1998)			Unsupervised (2018)		
SN	Class name	Area (ha)	Area (%)	Class name	Area (ha)	Area (%)
1	Agriculture	3907	27.17	Agriculture	3629	25.24
2	Built-up	48	0.33	Built-up	71	0.49
3	Forest	8617	59.92	Forest	7673	53.36
4	Wastelands	731	5.08	Wastelands	2714	18.87
5	Water bodies	1077	7.49	Water bodies	293	2.04
	Total	14380	100.00	Total	14380	100.00

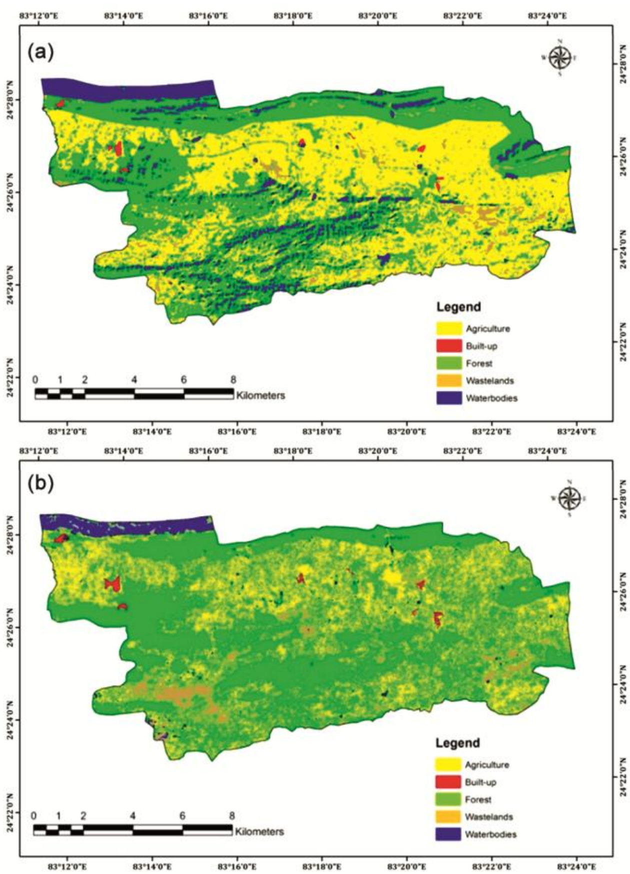

Fig. 3 — LULC classification using landsat data algorithm unsupervised (a) 1998 and (b) 2018

2018 (Table 2, Fig. 3). During this period, several water bodies might have been converted into agriculture and wasteland. The Forest cover have decreased by about 6.56% (944 ha) during this period. It was found that the forests might have been cut down by the locals for agriculture and built-up area (Fig. 4).

The urban fringe area grew from 0.33% (48 ha) in 1998 to 0.49% (71 ha) in 2018. Built-up areas are very important classes of LULC. The main cause of increase in built-up area is population growth. In this study, the Built-up area growth is not high (Table 2 and Fig. 3).

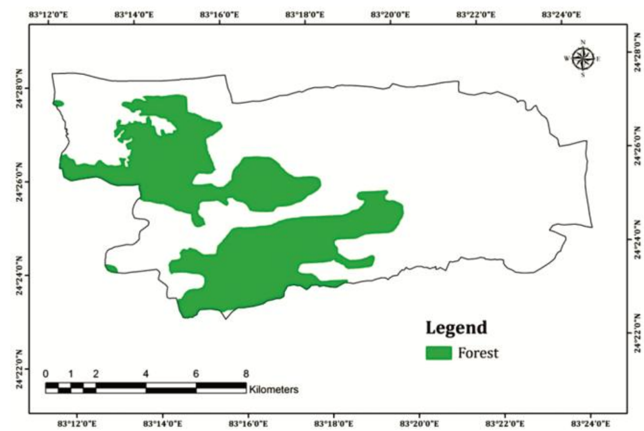

Fig. 4 — Forest in the study area of Ramgarh-Naudiha, Sonbhadra district

A large area of land that did not develop is the wasteland. The wasteland had increased fast from 5.08% (731 ha) in 1998 to 18.87% (2714 ha) in 2018, showing an increase by 13.79% (Table 2 & Fig. 3). It can be observed that the forest and agriculture lands have been converted into wastelands. This is one of the main reasons for conversion of the agricultural land and forest areas into wasteland.

Agriculture cover has gone down by 1.93% (278 ha) in 20 years from 27.17% in 1998. In 1998 the total agriculture area was 3907 ha and in 2018 was 3629 ha which may have happened due to lack of preplanning.

Accuracy Assessment

Remote sensing images need reference, or 'ground truthing' data to validate its accuracy assessment. Accuracy assessment by the 'traditional' methods is mostly difficult as it requires collection of ground truthing data simultaneously while detecting a change using numerous multi-temporal images. In this study, a new approach is proposed by assigning new rationality with appropriate post-classification comparison (Table 3).

User and Producer's accuracy were calculated separately on each type, such as, Water bodies, Agriculture, Forest, Built-up and Wastelands using

Table 3 — Accuracy assessment

Class Name		Ground truth: Water bodies	Agriculture	Forest	Built-up	Wastelands	No. of classified pixels
Classified image	Water bodies	**6**	1	0	0	1	8
	Agriculture	1	**10**	1	1	1	14
	Forest	0	1	**14**	1	1	17
	Built-up	0	1	1	**5**	1	8
	Wastelands	0	1	1	0	**5**	7
No. of ground truth pixels		7	14	17	7	9	**54**

Table 4 — Accuracy assessment

Class	Landsat-5 (1998) User accuracy (%)	Producer accuracy (%)	Overall accuracy (%)	Kappa (%)	Landsat-8 (2018) User accuracy (%)	Producer accuracy (%)	Overall accuracy (%)	Kappa
Water bodies	75.00	85.71	74.07	0.6649	85.71	66.67	80.00	0.7435
Agriculture	71.43	71.43			76.92	90.91		
Forest	82.35	82.35			87.50	93.33		
Built-up	62.50	71.43			71.43	71.43		
Wastelands	71.43	55.56			71.43	62.50		

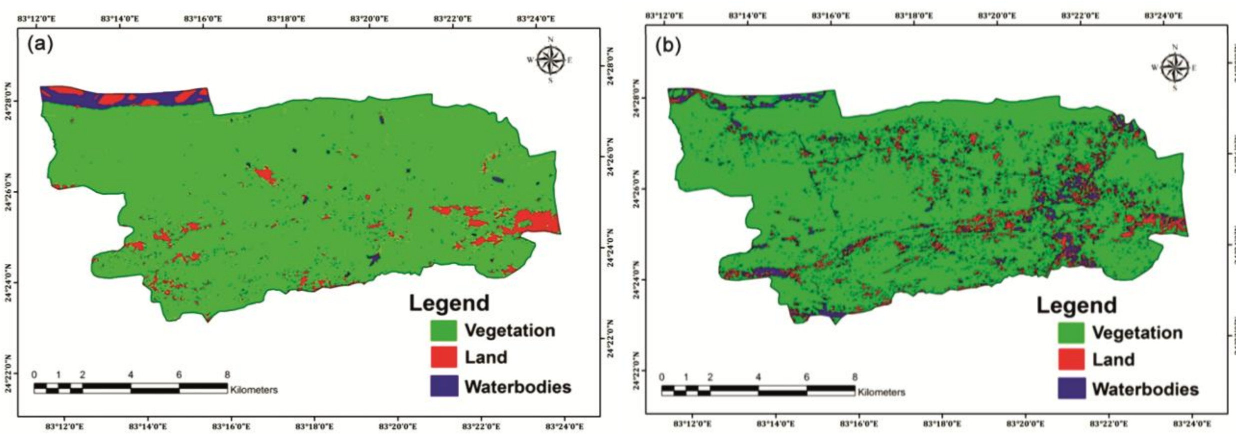

Fig. 5 — Normalised Difference Vegetation Index (NDVI) of the study area (a) 1998 and (b) 2018

Eqs (2–5). The calculated data of the study area from Landsat image in 1998 and 2018 (Table 3) show that in 1998 has 7 points as row total and column total as 8 points for Water bodies.

The accuracy of the calculated data for the year 1998 and 2018 is correct with errors within the acceptable limits (Table 4). The study area is highly vulnerable to natural calamities due to its geographic location. In this study, the calculated Water bodies have decreased by 5.45% from 1998 to 2018 (Table 2, Fig. 3). Change in forest cover is observed in remote sensing data using unsupervised analysis. Forest cover has decreased by about 6.56% from 1998 to 2018 (Table 2, Figs 3 & 4). The accuracy level of the NDVI results is 89%. Moreover, diachronic geospatial and non-spatial studies of change in forest area showed that LULC was conducted with different factors against time. Various causes of forest cover deterioration includes; poverty, population overgrowth, taboo felling, increased demand of agricultural land, lack of appropriate policy and its implementation.[34] Geospatial data on land cover showed that urban growth followed certain pattern between the 2000's and 2010's depending on the ground location and elevation.[35]

The study area has suffered quick LULC change due to fast population growth and urbanization that resulted severe contractions in agricultural land. The Producer's accuracy, User's Accuracy, Overall Accuracy and Kappa Coefficient have been calculated using Eqs 2–5 (Table 4).

Normalised Difference Vegetation Index (NDVI)

The NDVI values was in the range from –1 to 0.56 in 1998 image and in 2018 image the same ranges from –0.58 to 0.52 as calculated with the help of

ArcGIS 10.1. High NDVI value indicates high vegetation density.

The vegetation spread (Fig. 5) was 12524 ha in 1998 and 11302 ha in 2018 which indicate removal of 1222 ha vegetation cover within a span of 20 years. The high-density vegetation is relatively less affected. The ratio of red and near infrared bands from a remotely-sensed image gives NDVI on a per-pixel basis.

Conclusions

LULC change using remote sensing imagery has been studied in Ramgarh-Naudiha region of UP. The results demonstrate that LULC change produced a prominent negative impact on the biophysical indicators of environment in this study area which can be extrapolated from local to other similar areas. The rate of change of tree cover in a long term is useful threshold alarm for monitoring. Creation of fresh urban built-up is realized by engulfing agricultural land, vegetation and forest area. Water bodies and forests are converted into urban area because of population growth and development. The water bodies have also been filled up for urbanization purposes. This study provides vital indication on the changing scenario of LULC with developments and increases awareness. The NDVI data from the study shows that the medium and low-density vegetation are rapidly disappearing by the various anthropogenic causes in the study area while dense vegetation is less affected because of its high altitude. So LULC study utilising remote sensing data is very effective and useful for proper LULC planning and management.

Acknowledgements

The authors are extremely thankful to Director, CSIR-Central Glass & Ceramic Research Institute for permitting the study. The authors are thankful to AIGIRS, Noida for facilities provided and advise in preparation of this article. Thanks are also due to the Directorate of Geology and Mining, Government of Uttar Pradesh for providing important guidance of the area.

References

1 Amini S, Saber M, Rabiei-Dastjerdi H & Homayouni S, Urban land use and land cover change analysis using random forest classification of Landsat time series, *Remote Sens*, **14** (2022) 2654.

2 Mousivand A & Arsanjani J J, Insights on the historical and emerging global land cover changes: The case of ESA-CCI-LC datasets, *Appl Geogr*, **106** (2019) 82–92.

3 Harris N L, Brown S, Hagen, S C, Saatchi S S, Petrova S, Salas W, Hansen M C, Potapov P V & Lotsch A, Baseline map of carbon emissions from deforestation in tropical regions, *Science*, **336** (2012) 1573–1576.

4 Mahmood R, Pielke, R A & McAlpine C A, Climate-relevant land use and land cover change policies, *Bull Am Meteorol Soc*, **97** (2016) 195–202.

5 Mishra A & Pandey V K, Quantitative environmental impact assessment of the open cast mining in Sonbhadra district, Uttar Pradesh, India, *J Appl Nat Sci*, **5** (2013) 361–368.

6 Lin C, Tong X, Lu W, Yan L, Wu Y, Nie C, Chu C & Long J, Environmental impacts of surface mining on mined lands, affected streams and agricultural lands in the Dabaoshan mine region, Southern China, *Land Degrad Dev*, **16** (2005) 463–474.

7 Padmanaban R, Bhowmik A K & Cabral P, A remote sensing approach to environmental monitoring in a reclaimed mine area, *ISPRS Int J Geo-Inf*, **6** (2017) 401.

8 Firozjaei M K, Kiavarz M, Alavipanah S K, Lakes T & Qureshi S, Monitoring and forecasting heat island intensity through multi-temporal image analysis and cellular automata-markov chain modelling: A case of Babol City, Iran, *Ecol Indic*, **91** (2018) 155–170.

9 Butt A, Shabbir R, Ahmad S S & Aziz N, Land use change mapping and analysis using remote sensing and GIS: A case study of Simly watershed, Islamabad, Pakistan, *Egypt J Remote Sens Space Sci*, **18** (2015) 251–259.

10 Wang Z, Schaaf C B, Sun Q, Kim J H, Erb A M, Gao F, Román M O, Yang Y, Petroy S, Taylor J R, Masek J G, Morisette J T, Zhang X & Papuga S A, Monitoring land surface albedo and vegetation dynamics using high spatial and temporal resolution synthetic time series from Landsat and the MODIS BRDF/NBAR/Albedo product, *Int J Appl Earth Obs Geoinf*, **59** (2017) 104–117.

11 Weng Q, Lu D & Schubring J, Estimation of land surface temperature–vegetation abundance relationship for urban heat island studies, *Remote Sens Environ*, **89** (2004) 467–483.

12 Li H, Zhou Y, Li X, Meng L, Wang X, Wu S & Sodoudi S, A New method to quantify surface urban heat island intensity, *Sci Total Environ*, **624** (2018) 262–272.

13 Karmakar D, Singh V, Singh R, Sharma L K & Ghosh S, Beneficiation of clays from Ramgarh-Naudiha region of Sonbhadra District, Uttar Pradesh, impart improved properties for ceramic industries, *Ind J Eng Mater Sci*, **30** (2023) 65–72.

14 Lillesand T, Kiefer R W & Chipman J, *Remote sensing and image interpretation* (John Wiley & Sons, 7th Edn) 2015.

15 Shibi C S & Gayathri R, An efficient hardware implementation of detecting targets from remotely sensed hyperspectral images, *J Sci Ind Res*, **81** (2022) 156–165.

16 Navalgund R R, Remote Sensing 1. Basics and applications, *Resonance-J Sci Educ*, **6** (2001) 51–60.

17 Kunkel M L, Flores A N, Smith T J, McNamara J P & Benner S G, A simplified approach for estimating soil carbon and nitrogen stocks in semi-arid complex terrain, *Geoderma*, **165** (2011) 1–11.

18 Demirel H, Ozcinar C & Anbarjafari G, Satellite image contrast enhancement using discrete wavelet transform and singular value decomposition, *IEEE Geosci Remote Sens Lett*, **7** (2009) 333–337.

19 Malo A R & Nicholson S E, A Study of Rainfall and Vegetation Dynamics in the African Sahel using Normalized Difference Vegetation Index, *J Arid Environ*, **19** (1990) 1–24.
20 Schmidt H & Karnieli A, Remote sensing of the seasonal variability of vegetation in a semi-arid environment, *J Arid Environ*, **45** (2000) 43–59.
21 Tucker C J, Red and photographic infrared linear combinations for monitoring vegetation, *Remote Sens Environ*, **8** (1979) 127–150.
22 Karaburun A, Estimation of C Factor for Soil Erosion Modeling using NDVI in Buyukcekmece Watershed, *Ozean J Appl Sci*, **3** (2010) 77–85.
23 Ramachandra T & Kumar U, Geographic resources decision support system for land use, land cover dynamics analysis, in *Proc FOSS/GRASS Users Conf*, 2004 12–14.
24 Holben B N, Characteristics of maximum-value composite images from temporal AVHRR data, *Int J Remote Sens*, **7** (1986) 1417–1434.
25 Soufflet V, Tanré D, Begue A, Podaire A & Deschamps P, Atmospheric effects on NOAA AVHRR data over Sahelian regions, *Int J Remote Sens*, **12** (1991) 1189–1203.
26 Justice C O, Eck T, Tanre D & Holben B, The effect of water vapour on the normalized difference vegetation index derived for the Sahelian Region from NOAA AVHRR data, *Int J Remote Sens*, **12** (1991) 1165–1187.
27 Zha Y, Gao J & Ni S, Use of normalized difference built-up index in automatically mapping urban areas from tm imagery, *Int J Remote Sens*, **24** (2003) 583–594.
28 Tilahun A & Teferie B, Accuracy assessment of land use land cover classification using google earth, *Am J Environ Prot*, **4** (2015) 193–198.
29 Congalton R G, A review of assessing the accuracy of classifications of remotely sensed data, *Remote Sens Environ*, **37** (1991) 35–46.
30 Jensen J R & Cowen D C, Remote sensing of urban/suburban infrastructure and socio-economic attributes, *Photogramm Eng Remote Sens*, **65** (1999) 611–622.
31 Fung T & LeDrew E, For change detection using various accuracy, *Photogramm Eng Remote Sens*, **54** (1988) 1449–1454.
32 Chakravarty S, Ghosh S, Suresh C, Dey A & Shukla G, Deforestation?: causes, effects and control strategies, in *Global Perspectives on Sustainable Forest Management,* edited by C A Okia (IntechOpen) 2012, 1–26.
33 Mallupattu P K & Reddy J R S, Analysis of land use/land cover changes using remote sensing data and GIS at an urban area, Tirupati, India, *Sci World J*, **2013**, 268623.
34 Lambin E F, Turner B L, Geist H J, Agbola S B, Angelsen A, Bruce J W, Coomes O T, Dirzo R, Fischer G, Folke C, George P S, Homewood K, Imbernon J, Leemans R, Li X, Moran E F, Mortimore M, Ramakrishnan P S, Richards J F, Skanes H, Steffen W, Stone G D, Svedin U, Veldkamp T A, Vogel C & Xu J, The causes of land-use and land-cover change: moving beyond the myths, *Glob Environ Change*, **11** (2001) 261–269.
35 Rai R, Zhang Y, Paudel B, Li S & Khanal N R, A synthesis of studies on land use and land cover dynamics during 1930–2015 in Bangladesh, *Sustainability*, **9** (2017) 1866.